

# Latent Poisson models for networks with heterogeneous density

Tiago P. Peixoto\*

*Department of Network and Data Science, Central European University, H-1051 Budapest, Hungary  
ISI Foundation, Via Chisola 5, 10126 Torino, Italy and  
Department of Mathematical Sciences, University of Bath,  
Claverton Down, Bath BA2 7AY, United Kingdom*

Empirical networks are often globally sparse, with a small average number of connections per node, when compared to the total size of the network. However, this sparsity tends not to be homogeneous, and networks can also be locally dense, for example with a few nodes connecting to a large fraction of the rest of the network, or with small groups of nodes with a large probability of connections between them. Here we show how latent Poisson models that generate hidden multigraphs can be effective at capturing this density heterogeneity, while being more tractable mathematically than some of the alternatives that model simple graphs directly. We show how these latent multigraphs can be reconstructed from data on simple graphs, and how this allows us to disentangle disassortative degree-degree correlations from the constraints of imposed degree sequences, and to improve the identification of community structure in empirically relevant scenarios.

## I. INTRODUCTION

One of the most important properties of empirical networks — representing the pairwise interactions of social, biological, informational and technological systems — is that they exhibit a strong structural heterogeneity, while being globally sparse [1]. The latter property means that most possible connections between nodes are not observed, which as a consequence means that, on average, the probability of observing a connection between two nodes is very small, and hence the typical number of connections each node receives is much smaller than the total number of nodes in the network. For example, even though the global human population is in the order of billions, most people interact only with a far smaller number of other people. Nevertheless, such network systems are rarely *homogeneously* sparse: instead, local portions of the network can vary greatly in their number of interactions. As has been widely observed [2], the number of neighbors of each node is very often broadly distributed, typically spanning several orders of magnitude. In addition, networks exhibit diverse kinds of mixing patterns in relation to the degrees [3], e.g. nodes may connect to other nodes with similar degree (assortativity), or nodes with high degree may connect preferentially with nodes of low degree and vice-versa (disassortativity). It is possible also for networks to possess communities of tightly connected nodes [4], such that the probability of a link existing between members of these subgroups far exceeds the global average. The existence of such heterogeneous mixing patterns serves as a signature of the process responsible for the network formation and may give insight into its functional aspects.

A central complicating factor in the characterization and understanding of the different kinds of mixing patterns in networks is that they cannot be fully understood

in isolation. For example, although networks with degree heterogeneity can exhibit in principle any kind of mixing pattern, there is a stronger tendency of very heterogeneous networks to exhibit degree disassortativity [5–7]. This is because once the degrees of a fraction of the nodes become comparable to the total number of nodes in the network, there is no other option than to connect them with nodes of lower degree. Since it is not possible to fully decouple degree heterogeneity from mixing, it can become difficult to determine whether the latter is simply a byproduct of the former, or if it can be related to other properties of network formation.

The degree disassortativity induced from broad degree distributions can also occur in networks exhibiting community structure, and in a similar way: if a node has a degree comparable to the number of nodes in the community to which it belongs, it will tend to be connected to nodes of the same community with a smaller degree. The resulting mixing pattern may confuse community detection methods that do not account for this possibility, which will mistake the pattern that arises from a purely intrinsic constraint, with one that needs an extrinsic explanation in the form of a different division of the network into groups.

In this work we address the problem of describing degree and density heterogeneity by considering models of random multigraphs, i.e. where more than one link between nodes is allowed, as well as self-loops, following a Poisson distribution, where a full decoupling of the degree distribution and degree mixing patterns is in fact possible. These can be transformed into models of simple graphs by erasing self-loops and collapsing any existing multiedges into a single edges. Conversely, we can recover the decoupling of degree variability and mixing by *reconstructing* an underlying multigraph from a given observation of a simple graph. Then, by inspecting the inferred multigraph, we can finally determine what is cause and byproduct.

We also show how latent Poisson models can be employed in the task of community detection in the presence

---

\* peixotot@ceu.edu

of density and degree heterogeneity. When dealing with simple graphs, degree correction [8], as we show, is in general not sufficient to disentangle community structure from induced degree disassortativity. When performing latent multigraph reconstruction, we demonstrate that this becomes finally possible. Furthermore, we show how the latent multigraph approach is more effective at describing the heterogeneous density of many networks, when compared to just using a multigraph model directly to represent a simple graph, as is often done [9]. In particular, we show how this increases our ability to uncover smaller groups in large networks.

This paper is divided as follows. We begin in Sec. II by formalizing the intrinsic effect of degree constraints by employing the maximum-entropy principle, and we show how the Poisson model appears naturally when multiedge distinguishability is taken into consideration. In Sec. III we describe the erased Poisson model for simple graphs, we compare its induced degree correlations with alternative maximum-entropy models, and present methods of Bayesian inference capable of reconstructing it from simple graph data. We then show how it can shed light into the origins of degree disassortativity in empirical networks. In Sec. IV we show how the erased Poisson model can improve the task of community detection, by allowing the induced degree mixing to be decoupled from the modular network structure, and also describe arbitrary density heterogeneity, and thereby enhance the resolution of small dense communities in large globally sparse networks. We finalize in Sec. V with a conclusion.

## II. MAXIMUM-ENTROPY ENSEMBLES FOR SIMPLE AND MULTIGRAPHS

One of our primary objectives is to model the effects of degree heterogeneity in network structure. To this end, we will concern ourselves with network ensembles that satisfy the constraint that the expected degrees of the nodes are given as parameters. Specifically, if  $P(\mathbf{A})$  is the probability that network  $\mathbf{A}$  occurs in the ensemble, we have that the following condition needs to hold

$$\sum_{\mathbf{A}} P(\mathbf{A}) \sum_j A_{ji} = \hat{k}_i, \quad (1)$$

for a given expected degree sequence  $\hat{\mathbf{k}} = \{\hat{k}_1, \dots, \hat{k}_N\}$ , where  $A_{ij}$  determines the number of edges between nodes  $i$  and  $j$ ,  $k_i = \sum_j A_{ji}$  is the degree of node  $i$ , and  $N$  is the number of nodes in the network. Given the constraints of Eq. 1, there are many choices of ensemble  $P(\mathbf{A})$  that satisfy it. Since we want to understand the intrinsic effect of the imposed degrees on other aspects of the network structure, we are interested in the choice of  $P(\mathbf{A})$  that is maximally uniform, or agnostic, with respect to the possible networks, conditioned only that the above constraint is satisfied. More formally, this means we want the choice that maximizes the ensemble

entropy [10, 11]

$$\mathcal{S} = - \sum_{\mathbf{A}} P(\mathbf{A}) \ln P(\mathbf{A}). \quad (2)$$

Employing the method of Lagrange multipliers to perform the constrained maximization yields a product of independent distributions for each entry in the adjacency matrix,

$$P(\mathbf{A}) = \prod_{i < j} \frac{(\theta_i \theta_j)^{A_{ij}}}{Z_{ij}}, \quad (3)$$

where the  $\theta$  are ‘‘fugacities’’ (exponentials of Lagrange multipliers) that keep the constraints in place [5, 11–13], and  $Z_{ij} = \sum_{A_{ij}} (\theta_i \theta_j)^{A_{ij}}$  is a normalization constant, comprised of a sum over all possible values of  $A_{ij}$ . Thus, the value of  $Z_{ij}$  will be different depending on whether we are dealing with simple graphs or multigraphs. For the case of simple graphs with  $A_{ij} \in \{0, 1\}$ , we have  $Z_{ij} = 1 + \theta_i \theta_j$ , which results in independent Bernoulli distributions for every node pair,

$$P(\mathbf{A}) = \prod_{i < j} \frac{(\theta_i \theta_j)^{A_{ij}}}{1 + \theta_i \theta_j}, \quad (4)$$

with mean values

$$\langle A_{ij} \rangle = \frac{\theta_i \theta_j}{1 + \theta_i \theta_j}. \quad (5)$$

In order for the constraints of Eq. 1 to be fulfilled, the fugacities need to be chosen by solving the system of nonlinear equations

$$\sum_{j \neq i} \frac{\theta_i \theta_j}{1 + \theta_i \theta_j} = \hat{k}_i, \quad (6)$$

which in general does not admit closed analytical solutions, and needs to be solved numerically.

For multigraphs with  $A_{ij} \in \mathbb{N}_0$ , we have instead  $Z_{ij} = \sum_{A_{ij}=0}^{\infty} (\theta_i \theta_j)^{A_{ij}} = (1 - \theta_i \theta_j)^{-1}$ , assuming  $\theta_i \theta_j < 1$ , which results in a product of geometric distributions,

$$P(\mathbf{A}) = \prod_{i < j} (\theta_i \theta_j)^{A_{ij}} (1 - \theta_i \theta_j), \quad (7)$$

with mean values

$$\langle A_{ij} \rangle = \frac{\theta_i \theta_j}{1 - \theta_i \theta_j}, \quad (8)$$

and the fugacities are obtained by solving an analogous but different system of equations

$$\sum_{j \neq i} \frac{\theta_i \theta_j}{1 - \theta_i \theta_j} = \hat{k}_i, \quad (9)$$

which also cannot be solved in closed form in general.

In both of the above cases, if all imposed degrees  $\hat{k}_i$  are sufficiently smaller than  $\sqrt{2E}$ , with  $2E = \sum_i \hat{k}_i$  being twice the number of expected edges, then in the limit  $N \gg 1$  the fugacities can be obtained approximately as

$$\theta_i \approx \frac{\hat{k}_i}{\sqrt{2E}}. \quad (10)$$

In this case the expected value of the adjacency matrix becomes

$$\langle A_{ij} \rangle \approx \theta_i \theta_j = \frac{\hat{k}_i \hat{k}_j}{2E}, \quad (11)$$

both for simple and multigraphs, and hence the difference between those ensembles vanish. In this situation, the expected number of edges between nodes is in the order of  $1/N$ , for sparse networks with  $E \sim O(N)$ , and thus the networks are also locally sparse, since no portion of the network is connected with high probability. The ensemble does not possess intrinsic degree correlations between neighbors, since the expected value of the adjacency matrix is simply the product of the fugacities. However, if the expected degrees  $\hat{k}$  are broadly distributed, with a fraction of them approaching or exceeding  $\sqrt{2E}$  (known as the ‘‘structural cut-off’’ [14]), this assumption will no longer hold, even if the network is globally sparse with  $E \sim O(N)$ . In this situation, typical networks sampled from the ensemble will exhibit intrinsic nontrivial mixing patterns. We will return to this in Sec. III A, but for now we move to maximum-entropy ensembles with distinguishable multiedges.

### A. Distinguishable multiedges and the Poisson model

We now consider a third situation when multiple edges between nodes are allowed, but the individual edges between the same two nodes can be distinguished from one another. We do so by allowing the edges to belong to one of  $M$  discrete types. We implement this by introducing a binary variable  $X_{ij}^m \in \{0, 1\}$  specifying whether an edge of type  $m \in [1, M]$  exists between nodes  $i$  and  $j$ , such that the adjacency matrix of the associated multigraph becomes  $A_{ij} = \sum_{m=1}^M X_{ij}^m$ , so that  $A_{ij} \in [0, M]$ . By maximizing the entropy of this augmented ensemble while imposing the same degree constraints of Eq. 1, we obtain an equation similar in form to Eq. 3,

$$P(\mathbf{X}) = \prod_{i < j} \frac{(\theta_i \theta_j)^{\sum_m X_{ij}^m}}{Z_{ij}}, \quad (12)$$

but with a different normalization

$$Z_{ij} = \sum_{A_{ij}=0}^M \binom{M}{A_{ij}} (\theta_i \theta_j)^{A_{ij}} = (1 + \theta_i \theta_j)^M. \quad (13)$$

If we now consider the associated multigraph ensemble, by ignoring the edge types, we obtain a product of binomial distributions

$$\begin{aligned} P(\mathbf{A}) &= \sum_{\mathbf{X}} P(\mathbf{X}) \prod_{i < j} \delta_{A_{ij}, \sum_m X_{ij}^m} \\ &= \prod_{i < j} \binom{M}{A_{ij}} \left( \frac{\theta_i \theta_j}{1 + \theta_i \theta_j} \right)^{A_{ij}} \left( 1 - \frac{\theta_i \theta_j}{1 + \theta_i \theta_j} \right)^{M - A_{ij}}. \end{aligned} \quad (14)$$

Taking the limit  $M \rightarrow \infty$ , and making the variable transformation  $\theta_i \rightarrow \theta_i / \sqrt{M}$ , while keeping the constraints of Eq. 1 fixed, we obtain a product of Poisson distributions

$$P(\mathbf{A}) = \prod_{i < j} \frac{(\theta_i \theta_j)^{A_{ij}} e^{-\theta_i \theta_j}}{A_{ij}!}. \quad (16)$$

In this case the degree constraints take a simpler form

$$\hat{k}_i = \lim_{M \rightarrow \infty} \sum_{j \neq i} \frac{\theta_i \theta_j}{1 + \frac{\theta_i \theta_j}{M}} = \theta_i \sum_{j \neq i} \theta_j. \quad (17)$$

The above model becomes even more convenient if we allow for self-loops, i.e.  $A_{ii} > 0$ . Repeating the same calculations we obtain

$$P(\mathbf{A}) = \prod_{i < j} \frac{(\theta_i \theta_j)^{A_{ij}} e^{-\theta_i \theta_j}}{A_{ij}!} \prod_i \frac{(\theta_i^2/2)^{A_{ii}/2} e^{-\theta_i^2/2}}{(A_{ii}/2)!}, \quad (18)$$

where we adopt the convention that  $A_{ii}$  is twice the number of self-loops incident on node  $i$ . With this simple modification the degree constraints now become

$$\hat{k}_i = \theta_i \sum_j \theta_j. \quad (19)$$

Unlike any of the previous models considered, the above equations can be directly solved as

$$\theta_i = \frac{\hat{k}_i}{\sqrt{2E}}, \quad (20)$$

once more with  $2E = \sum_i \hat{k}_i$ . The mean of the adjacency entry is then

$$\langle A_{ij} \rangle = \theta_i \theta_j = \frac{\hat{k}_i \hat{k}_j}{\sqrt{2E}}. \quad (21)$$

This model, therefore, becomes asymptotically equivalent to the simple and multigraph ensembles considered previously if the expected degrees are all sufficiently smaller than  $\sqrt{2E}$ , however it retains a lack of intrinsic degree correlations even if this condition is not satisfied, since the expected number of edges between nodes is always a product of the fugacities. More specifically, the expected degree  $\langle k \rangle_{\text{nn}}(k)$  of the neighbors of nodes of degree  $k$  is given by

$$\langle k \rangle_{\text{nn}}(k) = \sum_{\mathbf{A}} P(\mathbf{A}) \frac{\sum_i \delta_{k_i, k} \sum_j A_{ji} k_j / k_i}{\sum_i \delta_{k_i, k}} \quad (22)$$

$$= \sum_i \theta_i^2 = \frac{\sum_i \hat{k}_i^2}{2E}, \quad (23)$$

which is a constant independent of  $k$ .

The Poisson model has been proposed originally by Norros and Reittu [15], but not as a maximum-entropy ensemble for multigraphs possessing distinguishable multiedges, as we do here. At first, this might seem like a construct designed primarily for mathematical convenience, rather than a principled proposition, as there is no inherent property of a multigraph that allows us to tell multiedges apart. However, there are situations where the notion of multiedge distinguishability does arise naturally. For example, there may be different roads between the same two cities [16], both of which are identifiable due to their spacial location. In proximity networks [17], multiedges correspond to events that are localized in space and time, and hence are distinguishable. We consider in Appendix A different kinds of intuitive random graph models that possess this property and show how they are exactly equivalent to the Poisson model. Nevertheless it generates multigraphs, where in many realistic settings we are interested in simple graphs, with at most one edge between two nodes.

A common approach is simply to ignore the discrepancy, and employ the Poisson model even when modeling simple graphs [8], arguing that the difference is negligible for sparse graphs, a point which we will examine in more detail in Sec. IV. For now, we simply anticipate that in order for this approximation to be valid, the graphs need to be *uniformly* sparse. In the following, we consider the erased Poisson model, which provides a better alternative to model simple graphs with heterogeneous sparsity.

### III. THE ERASED POISSON MODEL FOR SIMPLE GRAPHS

An alternative to the maximum-entropy model for simple graphs is the “erased” Poisson model, where a multigraph  $\mathbf{A}$  is generated from the Poisson model  $P(\mathbf{A}|\boldsymbol{\theta})$  and a simple graph  $\mathbf{G}(\mathbf{A})$  is obtained from it by simply ignoring (“erasing”) multiedge multiplicities and removing self-loops [18, 19], i.e.

$$G_{ij}(A_{ij}) = \begin{cases} 1 & \text{if } A_{ij} > 0 \text{ and } i \neq j, \\ 0 & \text{otherwise.} \end{cases} \quad (24)$$

The resulting simple graph  $\mathbf{G}$  is generated with probability

$$P(\mathbf{G}|\boldsymbol{\theta}) = \prod_{i < j} (1 - e^{-\theta_i \theta_j})^{G_{ij}} e^{-\theta_i \theta_j (1 - G_{ij})}, \quad (25)$$

and we can impose a desired expected degree sequence by solving the system of equations

$$\sum_{j \neq i} 1 - e^{-\theta_i \theta_j} = \hat{k}_i. \quad (26)$$

These equations also do not admit a general closed-form solution for  $\boldsymbol{\theta}$ . We therefore may ask if this model is

any more practical than the maximum-entropy variant of Eq. 4. As it turns out, it is, but before we see how, let us compare the properties of this model with the other ones we have seen so far.

#### A. Degree correlations

With the exception of the Poisson model, all other models considered yield samples with some form of degree-degree correlations. The difference between the ensembles can be seen by inspecting the average value of the adjacency matrix entries as a function of the product of the fugacities in each case, i.e.

$$\langle A_{ij} \rangle = \frac{\theta_i \theta_j}{1 + \theta_i \theta_j}, \quad (\text{Max-Ent simple graph})$$

$$= \frac{\theta_i \theta_j}{1 - \theta_i \theta_j}, \quad (\text{Max-Ent multigraph})$$

$$= \theta_i \theta_j, \quad (\text{Poisson multigraph})$$

$$\langle G_{ij} \rangle = 1 - e^{-\theta_i \theta_j}. \quad (\text{Erased Poisson simple graph})$$

These functions are illustrated in Fig. 1. For  $\theta_i \theta_j \ll 1$  all functions approach the same uncorrelated placement of edges as in the Poisson model with  $\langle A_{ij} \rangle \approx \theta_i \theta_j$ . For larger values the simple graph models show a saturation of the edge placement probability, which results in a disassortative degree correlation, as it prevents an excess of connections to nodes with larger fugacities. The maximum-entropy multigraph model, on the other hand, shows a divergence of the number of edges placed as  $\theta_i \theta_j \rightarrow 1$ , which results in an assortative degree correlation, due to the nonlinear accumulation of multiedges between nodes with high fugacity.<sup>1</sup> (We note that it is sometimes implied in the literature that multigraph ensembles are uncorrelated. This is only true for models where multiedges are distinguishable, such as the Poisson and configuration models, not otherwise.)

For the Poisson multigraph model, the purely linear dependence on the fugacities implies a total lack of correlations between degrees at the endpoints of each edge, as we have already seen. The situation changes when multigraphs are erased, where we observe a similar, although not identical, saturation in the edge placement

<sup>1</sup> This multiedge concentration is reminiscent of the Bose-Einstein condensation phenomenon in quantum physics, where the number of particles in the ground state of a Bose gas diverges in a similar way. Indeed, Eq. 5 for simple graphs and Eq. 8 for multigraphs follow the Fermi-Dirac and Bose-Einstein statistics, respectively. Following this analogy, the uniformly sparse graph regime where both ensembles agree would correspond to the classical Maxwell-Boltzmann statistics, valid for low densities or high temperatures. The Poisson multigraph model can be interpreted as an extension of this classical limit to arbitrary densities. We note however that, in network science, Bose-Einstein condensation is more commonly associated with a different phenomenon of growing networks [20].

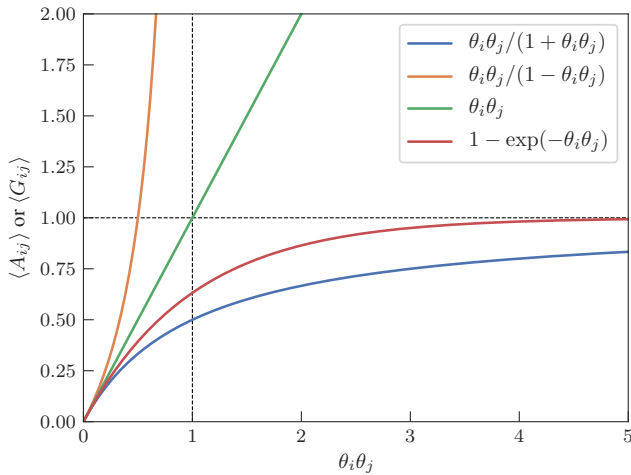


Figure 1. Average number of edges between nodes as a function of the product of their fugacities, for the different ensembles, as shown in the legend.

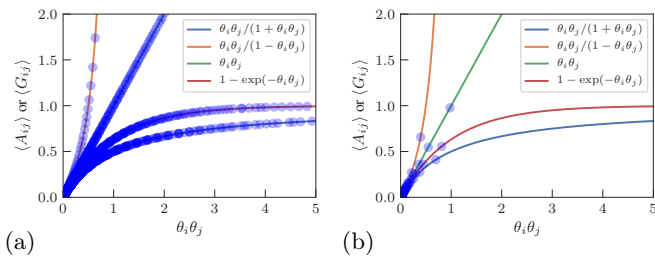


Figure 2. The same as Fig. 1, but showing the values for the edges of samples of each model with  $N = 10^6$  nodes, and with the same set of imposed degrees sampled from the Zipf distribution of Eq. 27, using (a)  $\alpha = 2.2$  and (b)  $\alpha = 2.4$ .

probability, which also results in a disassortative degree-degree correlation among neighbors.

The difference between the ensembles can be further illustrated by choosing integer-valued imposed degrees that are independently sampled from a Zipf distribution

$$P(k|\alpha) = \frac{k^{-\alpha}}{\zeta(\alpha)}, \quad (27)$$

with  $\zeta(\alpha)$  being the Riemann zeta function. For values of  $\alpha \in [2, 3]$  the variance of this distribution diverges, while the mean remains finite, therefore serving as a simple model of globally sparse but locally dense networks. In Fig. 2 we show how the edges present in one sample of each model are distributed along the curves of Fig. 1: A smaller value of  $\alpha$  creates broader and denser networks, for which the discrepancy between all models is very large. Although the mean degree of the generated networks in the case  $\alpha = 2.2$  is only around 3.75, even on a network of  $N = 10^6$  nodes the probability of observing an edge between two nodes approaches one for a significant number of pairs. As the exponent  $\alpha$  increases, the network becomes more homogeneously sparse, and the

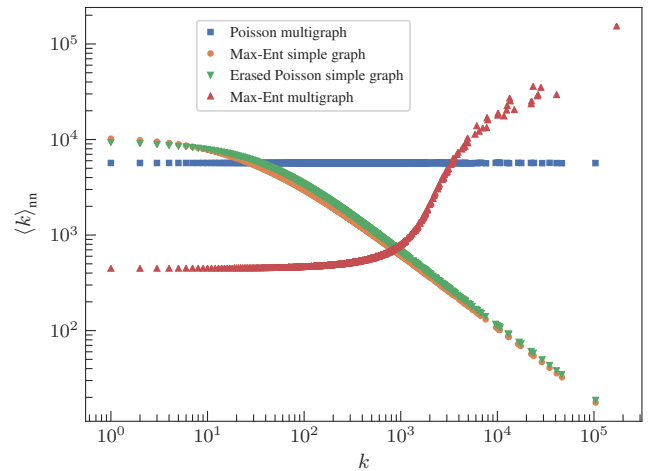


Figure 3. Mean degree of a neighbor of a node of degree  $k$ , as a function of  $k$ ,  $\langle k \rangle_{nn}(k)$ , for the different ensembles considered, with  $N = 10^6$  and the same set of imposed degrees sampled from Eq. 27 with  $\alpha = 2.2$ . (The error bars on the  $\langle k \rangle_{nn}$  values are smaller than the symbols used.)

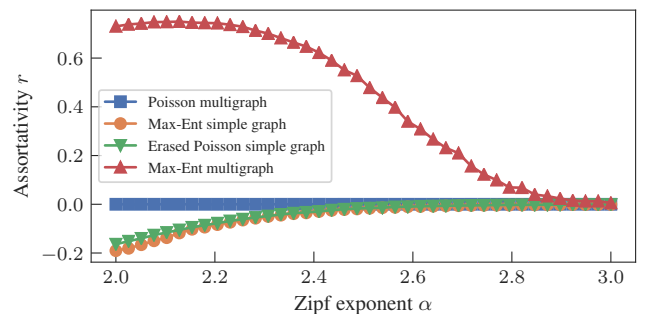


Figure 4. Degree assortativity  $r$  as a function of the Zipf exponent  $\alpha$ , for networks with  $N = 10^6$  nodes sampled from the models indicated in the legend.

fugacities and corresponding edge probabilities become more similar across ensembles.

The induced degree correlations among neighbors in each ensemble are shown in Fig. 3, in each case for the same set of imposed degrees sampled from Eq. 27. Some aspects of the degree correlations of the erased Poisson model were considered rigorously in Refs. [21, 22], and in the case of the maximum-entropy simple graph model in Ref. [5]. One important point to notice is that, although the erased Poisson and maximum-entropy models for simple graphs are not identical, they generate a very similar disassortative trend, indicating a comparable explanatory power for this kind of effect.

A further comparison is seen in Fig. 4 where the degree assortativity coefficient [3]  $r \in [-1, 1]$  is shown as a function of the Zipf exponent  $\alpha$ , defined as

$$r = \frac{\sum_{kk'} kk' (m_{kk'} - q_k q_{k'})}{\sigma_k^2}, \quad (28)$$

with  $m_{kk'} = \sum_{ij} A_{ij} \delta_{k_i, k} \delta_{k_j, k'} / 2E$  being the fraction of edges between nodes of degrees  $k$  and  $k'$ ,  $q_k = \sum_{k'} m_{kk'}$  is distribution of degrees at the endpoints of edges, and  $\sigma_k^2$  is its variance. We see that the same pattern persists for the entire range of  $\alpha \in [2, 3]$ , with the assortativity values being very similar between the erased Poisson and maximum-entropy simple graph models.

The similarity between the erased Poisson and the maximum-entropy simple graph model makes the former attractive as an alternative, considering its flexibility, as we are about to explore in the next section.

## B. Reconstructing the erased Poisson model

The ensembles considered previously translate different assumptions about the data into probability distributions, conditioned on desired constraints, and mediated by the maximum-entropy ansatz. In principle we should choose the set of assumptions that most closely matches the data in question.

Although we have argued that the Poisson model is well motivated in situations where multiedges can be distinguished, for simple graphs in particular there is a practical advantage to using the erased Poisson model, regardless if it is truly the most adequate mechanistic explanation or null model. Namely, it allows us to disentangle the edge placement from the inherent degree correlations, since the latter is only caused by the erasing of multiedges, and is absent from the original multigraph. We can do the same even if we only have the final simple graph at our disposal, by attempting to reconstructing the multigraph that generated it. If the latent multigraph does not exhibit degree correlations, we can conclude those were caused by the erasure procedure — which simply reflects the inherent constraints of having to generate a simple graph, and not some extrinsic propensity of high-degree nodes to connect to low-degree ones.

In the following we describe a principled and efficient method to perform such a reconstruction. We approach the task in a Bayesian way, by considering the posterior distribution of multigraphs  $\mathbf{A}$  and fugacities  $\boldsymbol{\theta}$  conditioned on an observed simple graph  $\mathbf{G}$ ,

$$P(\mathbf{A}, \boldsymbol{\theta} | \mathbf{G}) = \frac{P(\mathbf{G} | \mathbf{A}) P(\mathbf{A} | \boldsymbol{\theta}) P(\boldsymbol{\theta})}{P(\mathbf{G})}, \quad (29)$$

with  $P(\mathbf{G} | \mathbf{A})$  given by

$$P(G_{ij} | A_{ij}) = \begin{cases} 1, & \text{if } G_{ij} = G_{ij}(A_{ij}), \\ 0, & \text{otherwise,} \end{cases} \quad (30)$$

with  $G_{ij}(A_{ij})$  given by Eq. 24 and with  $P(\mathbf{A} | \boldsymbol{\theta})$  being the Poisson multigraph model of Eq. 16. The distribution  $P(\boldsymbol{\theta})$  is our prior for the fugacities, which for the moment we will assume to be constant  $P(\boldsymbol{\theta}) \propto 1$ , meaning we are fully agnostic about what kind of model generated the

data (we will revisit this assumption in Sec. IV). Finally, we have the so-called evidence

$$P(\mathbf{G}) = \sum_{\mathbf{A}} \int P(\mathbf{G} | \mathbf{A}) P(\mathbf{A} | \boldsymbol{\theta}) P(\boldsymbol{\theta}) d\boldsymbol{\theta}, \quad (31)$$

which is an unimportant constant for our present purpose. With the posterior distribution  $P(\mathbf{A}, \boldsymbol{\theta} | \mathbf{G})$  in place, we can proceed in a variety of ways, for example by sampling from it using MCMC. But instead, we will proceed in a more efficient manner, by considering first the most likely fugacities, when averaged over all possible multigraphs  $\mathbf{A}$ , i.e.

$$\hat{\boldsymbol{\theta}} = \operatorname{argmax}_{\boldsymbol{\theta}} \sum_{\mathbf{A}} P(\mathbf{A}, \boldsymbol{\theta} | \mathbf{G}) = \operatorname{argmax}_{\boldsymbol{\theta}} P(\mathbf{G} | \boldsymbol{\theta}), \quad (32)$$

where  $P(\mathbf{G} | \boldsymbol{\theta})$  is the erased Poisson likelihood of Eq. 25. Noting that taking the logarithm of the likelihood does not alter the position of its maximum, and substituting leads to

$$\hat{\boldsymbol{\theta}} = \operatorname{argmax}_{\boldsymbol{\theta}} \sum_{i < j} G_{ij} \ln(1 - e^{-\theta_i \theta_j}) - (1 - G_{ij}) \theta_i \theta_j. \quad (33)$$

Taking the derivatives of the right hand side with respect to  $\boldsymbol{\theta}$  and setting them to zero yields a system of nonlinear implicit equations that does not admit an obvious solution in closed form in the general case. Fortunately, we can obtain a simple algorithm for solving it, by slightly augmenting our problem, and obtaining at the same time a conditional posterior distribution over multigraphs  $P(\mathbf{A} | \mathbf{G}, \hat{\boldsymbol{\theta}})$ . We do so by employing Jensen's inequality on  $P(\mathbf{G} | \boldsymbol{\theta}) = \sum_{\mathbf{A}} P(\mathbf{G} | \mathbf{A}) P(\mathbf{A} | \boldsymbol{\theta})$  in the form

$$\ln \sum_{\mathbf{A}} P(\mathbf{G} | \mathbf{A}) P(\mathbf{A} | \boldsymbol{\theta}) \geq \sum_{\mathbf{A}} q(\mathbf{A}) \ln \frac{P(\mathbf{G} | \mathbf{A}) P(\mathbf{A} | \boldsymbol{\theta})}{q(\mathbf{A})}, \quad (34)$$

where the equality is achieved by setting

$$q(\mathbf{A}) = \frac{P(\mathbf{G} | \mathbf{A}) P(\mathbf{A} | \boldsymbol{\theta})}{\sum_{\mathbf{A}'} P(\mathbf{G} | \mathbf{A}') P(\mathbf{A}' | \boldsymbol{\theta})} = P(\mathbf{A} | \mathbf{G}, \boldsymbol{\theta}), \quad (35)$$

$$= \prod_{i < j} P(A_{ij} | G_{ij}, \boldsymbol{\theta}), \quad (36)$$

which is precisely the posterior distribution of multigraphs conditioned on a particular choice of fugacities, whose entries can be directly computed as

$$P(A_{ij} | G_{ij}, \boldsymbol{\theta}) = \begin{cases} \frac{\theta_i \theta_j^{A_{ij}} e^{-\theta_i \theta_j} \frac{1 - \delta_{A_{ij}, 0}}{A_{ij}!} \frac{1 - e^{-\theta_i \theta_j}}{1 - e^{-\theta_i \theta_j}}}{(\theta_i^2 / 2)^{A_{ii}/2} e^{-\theta_i^2 / 2} (A_{ii}/2)!} & \text{if } G_{ij} = 1, \\ & \text{if } i = j, \\ 0 & \text{otherwise.} \end{cases} \quad (37)$$

It will be useful to summarize this posterior distribution via its mean value for each node pair, given by

$$w_{ij} \equiv \langle A_{ij} \rangle = \begin{cases} \frac{\theta_i \theta_j}{1 - e^{-\theta_i \theta_j}} & \text{if } G_{ij} = 1, \\ \theta_i^2 & \text{if } i = j, \\ 0 & \text{otherwise.} \end{cases} \quad (38)$$

With this at hand, we then return to the maximization to obtain

$$\hat{\theta} = \operatorname{argmax}_{\theta} \sum_{\mathbf{A}} q(\mathbf{A}) \ln \frac{P(\mathbf{G}|\mathbf{A})P(\mathbf{A}|\theta)}{q(\mathbf{A})} \quad (39)$$

$$= \operatorname{argmax}_{\theta} \sum_{i \leq j} \sum_{A_{ij}=0}^{\infty} q(A_{ij}) \ln P(A_{ij}|\theta) \quad (40)$$

$$= \operatorname{argmax}_{\theta} \frac{1}{2} \sum_{ij} w_{ij} \ln \theta_i \theta_j - \theta_i \theta_j. \quad (41)$$

The last equation can be solved easily, which yields

$$\hat{\theta}_i = \frac{d_i}{\sqrt{\sum_j d_j}}, \quad (42)$$

where

$$d_i = \sum_j w_{ji} \quad (43)$$

is the expected degree of node  $i$  in the multigraph  $\mathbf{A}$ , averaged over  $P(\mathbf{A}|\mathbf{G}, \hat{\theta})$ . Since we are interested in the self-consistent values of  $\mathbf{w}$  conditioned on  $\hat{\theta}$ , this leads us to the following expectation-maximization (EM) algorithm, which starts with some arbitrary choice of  $\theta$ , and alternates between the following steps

1. In the ‘‘expectation’’ step we obtain the marginal mean multiedge multiplicities via:

$$w_{ij} = \begin{cases} \frac{\theta_i \theta_j}{1 - e^{-\theta_i \theta_j}} & \text{if } G_{ij} = 1, \\ \theta_i^2 & \text{if } i = j, \\ 0 & \text{otherwise.} \end{cases} \quad (44)$$

2. In the ‘‘maximization’’ step we use the current values of  $\mathbf{w}$  to update the values of  $\theta$ :

$$\theta_i = \frac{d_i}{\sqrt{\sum_j d_j}}, \quad \text{with } d_i = \sum_j w_{ji}. \quad (45)$$

Upon convergence, the above EM algorithm is guaranteed to find only a local optimum of the maximization problem, therefore we may need to run it multiple times with different initial choices of  $\theta$ . However, in all our experiments we found that the algorithm tends to find the same solution from any initial starting point, even when this happens to be the correct solution (in artificially generated examples where this is known), giving strong evidence that the global optimum is usually found. This algorithm is efficient, since we need only to keep track of the values for  $\mathbf{w}$  for the observed edges in  $\mathbf{G}$ , in addition to each self-loop. Therefore the E-step can be done in  $O(E + N)$  time, and the M-step in  $O(N)$  time, resulting in an overall  $O(E + N)$  computational complexity. The algorithm can also be run in parallel easily. The number of EM iterations required for convergence depends on the

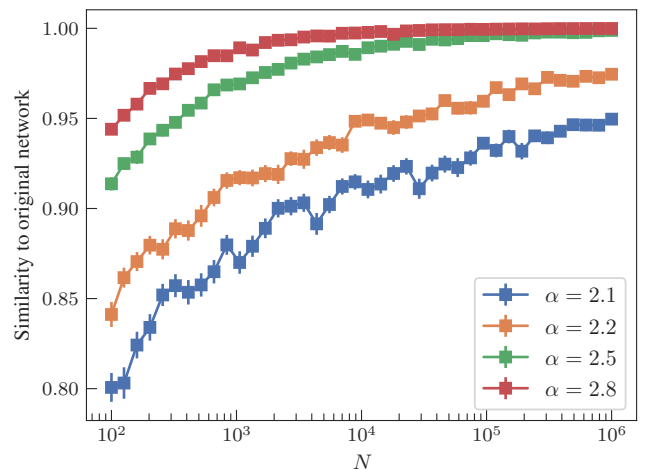


Figure 5. Poisson multigraph reconstruction accuracy as measured via the similarity of Eq. 46 for simple graphs sampled from the erased Poisson model with imposed degrees sampled from a Zipf distribution with exponent  $\alpha$ , as a function of the number of nodes  $N$ . Each point was averaged over 100 realizations.

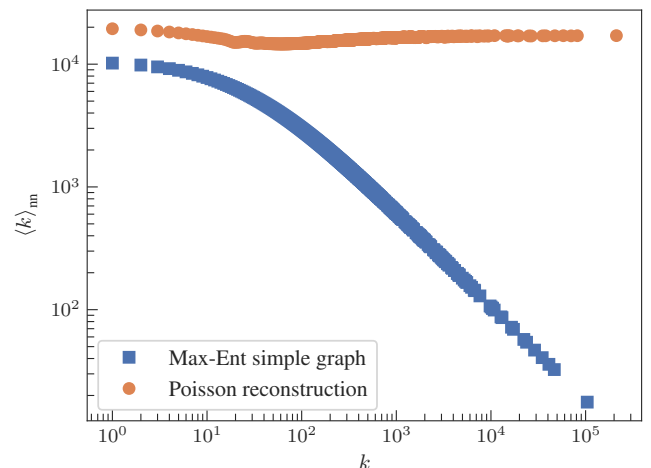


Figure 6. Mean degree of a neighbor of a node of degree  $k$ , as a function of  $k$ , for a network with  $N = 10^6$  nodes sampled from the maximum-entropy ensemble with imposed degrees sampled from Eq. 27 with  $\alpha = 2.2$ , and its inferred Poisson multigraph, using the algorithm described in the text.

data and initial conditions, but we have successfully run it on networks with up to  $10^8$  edges on a regular laptop computer. Our C++ implementation of the above algorithm is available as part of the `graph-tool` Python library [23].

In Fig. 5 we show how the algorithm behaves in recovering the underlying multigraph of artificial networks sampled from the erased Poisson model, as measured via

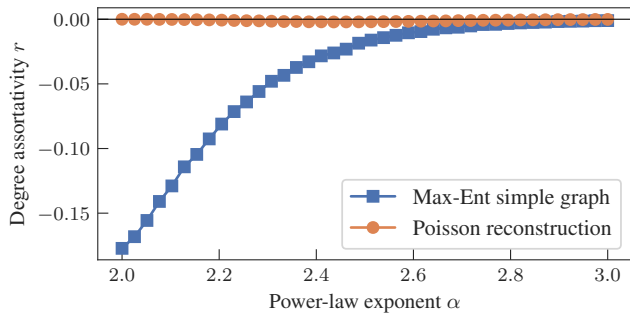


Figure 7. Degree assortativity as function of the Zipf exponent  $\alpha$ , for networks with  $N = 10^6$  nodes sampled from the maximum entropy ensemble with Zipf-distributed imposed degrees, and their corresponding inferred Poisson multigraphs.

the Jaccard similarity

$$s(\mathbf{w}, \mathbf{A}) = 1 - \frac{\sum_{ij} |w_{ij} - A_{ij}|}{\sum_{ij} w_{ij} + A_{ij}} \quad (46)$$

between the true and inferred multigraphs, with imposed degrees sampled from a Zipf distribution. For smaller values of the exponent  $\alpha$ , which causes the edge multiplicities to become larger, the recovery becomes less accurate, but in all cases it approaches  $s(\mathbf{w}, \mathbf{A}) \rightarrow 1$  as the number of nodes increases, indicating that full recovery is possible asymptotically as the amount of available data increases.

Since this algorithm gives us a distribution over multigraphs, we can use it to investigate whether the degree correlations of an observed simple graphs exist as a necessary outcome of the existing degrees, or if they should be attributed to something else. In the first scenario, the degree-degree correlations would disappear in the inferred multigraph, whereas they would persist in the second one. Interestingly, this works reasonably well even when the observed graph was not sampled from the erased Poisson model. We illustrate this with an example in Fig. 6, where a simple graph was generated from a maximum-entropy model with Zipf-distributed degrees, and we inferred from it a corresponding Poisson multigraph. Even though the inferred multigraph still shows a weak degree correlation between neighboring nodes, since the erased Poisson model cannot fully account for the structure of the maximum-entropy model, the overall disassortative trend is completely absent. Fig. 7 shows the degree assortativity values for both original and reconstructed networks over a range of  $\alpha \in [2, 3]$ . Although the reconstructed networks still show values  $r < 0$ , their deviation from zero is barely noticeable in the figure. Like we had seen previously in Fig. 3, these results further show that the erased Poisson model generates mixing patterns that, although not identical, are sufficiently similar to the maximum-entropy simple graph model, allowing us to correctly conclude that the resulting degree correlations arise directly from the imposed degrees.

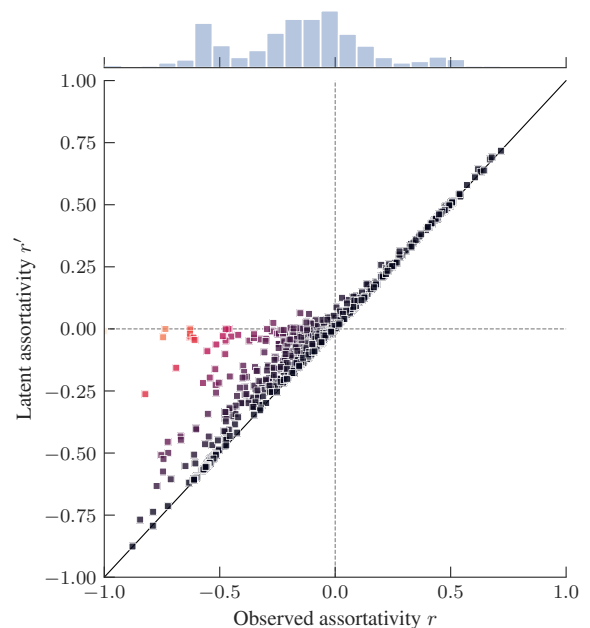


Figure 8. Degree assortativity for original simple graph  $r$ , and for the reconstructed multigraph  $r'$  for 816 empirical networks, obtained from the CommunityFitNet [24] and Konect [25] databases.

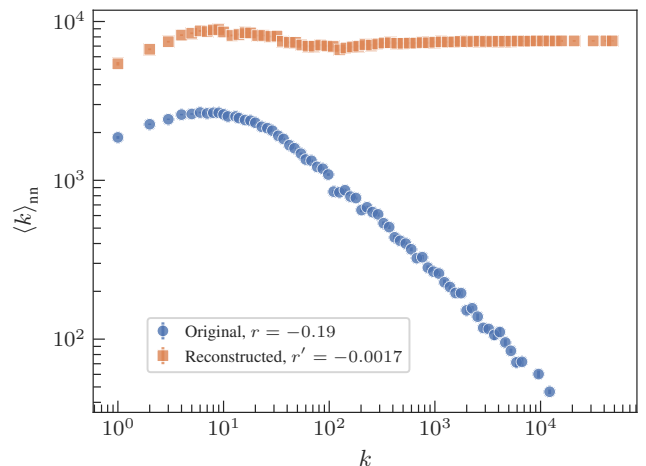


Figure 9. Mean degree of a neighbor of a node of degree  $k$  as a function of  $k$ , for the internet at the autonomous systems level, both for the original network and reconstructed multigraph, as shown in the legend, which includes the degree assortativity coefficient of each case.

### C. Empirical networks

We can use the erased Poisson model to decouple degree assortativity from the degree constraints by inferring the underlying multigraph where these properties are not tied to each other. In Fig. 8 we show the results of applying our algorithm to 816 networks across differ-

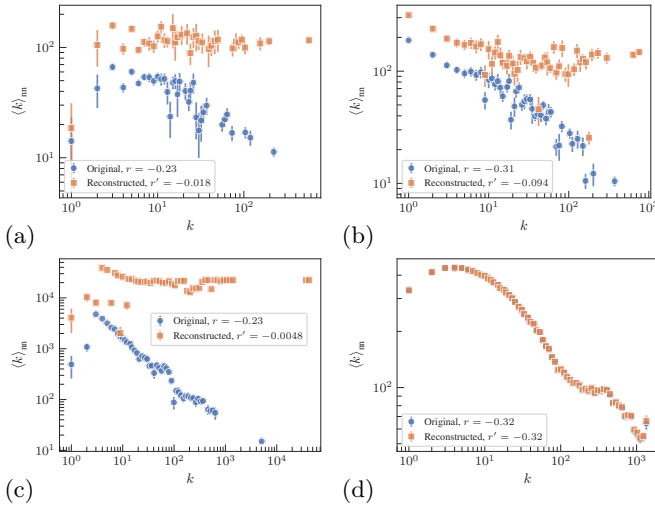


Figure 10. Mean degree of a neighbor of node of degree  $k$  as a function of  $k$ , for (a) the metabolic network of *C. elegans* [26], (b) the network of leaked emails of the Democratic National Committee, (c) the class dependency graph of a large software project [27], and (d) the online social network Flixter [28], both for the original network and reconstructed multigraph, as shown in the legend, which includes the degree assortativity coefficient of each case.

ent domains, obtained from the CommunityFitNet [24] and Konect [25] databases, and comparing the assortativity coefficient computed for the original network and reconstructed multigraph. For assortative mixing patterns with  $r > 0$  we do not observe any significant difference, as this kind of mixing pattern is unrelated to degree constraints. However, for disassortative values  $r < 0$  we observe a variety of behaviors, where for many networks the assortativity value is significantly increased in the reconstructed multigraph, indicating that observed correlations can be largely associated with the broadness of the degrees. A prime example of this is the Internet at the autonomous systems level [29], which has been long considered as a case where the observed disassortativity is a byproduct of the broad degree sequence rather than an independent feature of the network [5, 30]. As we see in Fig. 9, we can recover this result clearly with our reconstruction method, where the inferred multigraph completely lacks the disassortativity pattern. Other examples of this phenomenon are shown in Fig. 10 for the metabolic network of *C. elegans* [26], the network of leaked emails of the Democratic National Committee, and the class dependency graph of a large software project [27]. We also show the reconstruction results for the now-extinct online social network Flixter [28], where users could share their taste on films. This network displays a strong degree disassortativity which persists completely in the reconstructed Poisson multigraph, indicating that it does not in fact arise from the inherent constraints of the existing degrees, and must therefore be due to some other mechanism.

#### IV. COMMUNITY DETECTION

Another important type of heterogeneous sparsity is community structure [4], which can be loosely defined as the existence of groups of nodes with a high probability of connection to themselves, or also to other groups. Models for networks with this kind of structure can be obtained by forcing the number of edges between groups to have specific values. More precisely, we assume the nodes are divided into  $B$  disjoint groups, with  $b_i \in [1, B]$  denoting the group membership of node  $i$ . With this, and in addition to the expected degree constraints, we have the expected edge counts between groups given by

$$\sum_{\mathbf{A}} P(\mathbf{A}) \sum_{ij} A_{ij} \delta_{b_i, r} \delta_{b_j, s} = m_{rs}. \quad (47)$$

Performing the same calculation as before, i.e. maximizing the ensemble entropy conditioned on the above constraints in addition to Eq. 1 we arrive at the model

$$P(\mathbf{A}|\boldsymbol{\lambda}, \boldsymbol{\theta}, \mathbf{b}) = \prod_{i < j} \frac{(\lambda_{b_i b_j} \theta_i \theta_j)^{A_{ij}}}{\lambda_{b_i b_j} \theta_i \theta_j + 1}, \quad (48)$$

in the case of simple graphs, which contains another set of fugacities  $\boldsymbol{\lambda}$ . The values of the fugacities  $\boldsymbol{\theta}$  and  $\boldsymbol{\lambda}$  are determined by solving the following set of equations

$$\sum_{j \neq i} \frac{\lambda_{b_i b_j} \theta_i \theta_j}{\lambda_{b_i b_j} \theta_i \theta_j + 1} = \hat{k}_i, \quad \sum_{ij} \frac{\lambda_{rs} \theta_i \theta_j \delta_{b_i, r} \delta_{b_j, s}}{\lambda_{rs} \theta_i \theta_j + 1} = m_{rs}, \quad (49)$$

which once more cannot be solved in closed form.

Instead, if we consider multigraphs with distinguishable multiedges, performing the same calculations as before, we arrive at the Poisson version of the degree-corrected SBM (DC-SBM), originally proposed by Karrer and Newman [8]

$$P(\mathbf{A}|\boldsymbol{\lambda}, \boldsymbol{\theta}, \mathbf{b}) = \prod_{i < j} \frac{(\lambda_{b_i b_j} \theta_i \theta_j)^{A_{ij}} e^{-\lambda_{b_i b_j} \theta_i \theta_j}}{A_{ij}!} \times \prod_i \frac{(\lambda_{b_i b_i} \theta_i^2 / 2)^{A_{ii}/2} e^{-\lambda_{b_i b_i} \theta_i^2 / 2}}{(A_{ii}/2)!}. \quad (50)$$

As pointed out in Ref. [8], this model is more tractable, and we can obtain the fugacities directly as

$$\theta_i = \frac{\hat{k}_i}{\sum_j \hat{k}_j \delta_{b_j, b_i}}, \quad \lambda_{rs} = m_{rs}. \quad (51)$$

Rather than the fugacities, in this context we are primarily interested in obtaining the partition  $\mathbf{b}$  given an observed network  $\mathbf{A}$ , hence we focus on the posterior

$$P(\mathbf{b}|\mathbf{A}) = \frac{P(\mathbf{A}|\mathbf{b})P(\mathbf{b})}{P(\mathbf{A})}, \quad (52)$$

with the marginal likelihood being integrated over the fugacities

$$P(\mathbf{A}|\mathbf{b}) = \int P(\mathbf{A}|\boldsymbol{\lambda}, \boldsymbol{\theta}, \mathbf{b})P(\boldsymbol{\theta}|\mathbf{b})P(\boldsymbol{\lambda}|\mathbf{b}) d\boldsymbol{\theta}d\boldsymbol{\lambda}, \quad (53)$$

If we use noninformative priors

$$P(\boldsymbol{\theta}|\mathbf{b}) = \prod_r (n_r - 1)! \delta(\sum_i \theta_i \delta_{b_i, r} - 1), \quad (54)$$

$$P(\boldsymbol{\lambda}|\mathbf{b}, \bar{\lambda}) = \prod_{r < s} e^{-\lambda_{rs}/\bar{\lambda}} / \bar{\lambda} \prod_r e^{-\lambda_{rs}/2\bar{\lambda}} / 2\bar{\lambda}, \quad (55)$$

we can compute the integral for the Poisson model as [31]

$$P(\mathbf{A}|\mathbf{b}) = \frac{\bar{\lambda}^E}{(\bar{\lambda} + 1)^{E+B(B+1)/2}} \times \frac{\prod_{r < s} e_{rs}! \prod_r e_{rr}!!}{\prod_{i < j} A_{ij}! \prod_i A_{ii}!!} \times \prod_r \frac{(n_r - 1)!}{(e_r + n_r - 1)!} \prod_i k_i!, \quad (56)$$

where  $e_{rs} = \sum_{ij} A_{ij} \delta_{b_i, r} \delta_{b_j, s}$ , and  $e_r = \sum_s e_{rs}$ . Although there are good reasons not to use such uninformative priors [31], the above calculation illustrates how the Poisson model allows us to perform computations that would be very difficult with the maximum-entropy model. Going further, and exploiting the equivalence with the microcanonical configuration model as was shown in Ref. [31], it is possible to replace these priors by nested sequences of priors and hyperpriors that enhance our capacity to identify small groups in large networks, more adequately describe broad degree sequences, and uncover hierarchical modular structures.

Despite these advantages, the Poisson DC-SBM model inherits all the shortcomings of the Poisson model we considered previously, when applied to simple graph data. In order to alleviate these problems, we may therefore also employ the erased Poisson model for community detection, with a likelihood

$$P(\mathbf{G}|\boldsymbol{\lambda}, \boldsymbol{\theta}, \mathbf{b}) = \prod_{i < j} (1 - e^{-\lambda_{b_i b_j} \theta_i \theta_j})^{G_{ij}} e^{-\lambda_{b_i b_j} \theta_i \theta_j (1 - G_{ij})}. \quad (57)$$

This likelihood, however, makes the direct computation of the marginal likelihood intractable, as it is not easy to perform the integral over  $\boldsymbol{\lambda}$  and  $\boldsymbol{\theta}$ . Instead, we proceed in a different manner, by considering the joint likelihood of the simple graph  $\mathbf{G}$  and its underlying multigraph  $\mathbf{A}$ ,

$$P(\mathbf{G}, \mathbf{A}|\boldsymbol{\lambda}, \boldsymbol{\theta}, \mathbf{b}) = P(\mathbf{G}|\mathbf{A})P(\mathbf{A}|\boldsymbol{\lambda}, \boldsymbol{\theta}, \mathbf{b}), \quad (58)$$

with  $P(\mathbf{G}|\mathbf{A})$  given by Eq. 30. In this manner, we can easily write the joint posterior distribution over the node partition and multigraph

$$P(\mathbf{A}, \mathbf{b}|\mathbf{G}) = \frac{P(\mathbf{G}|\mathbf{A})P(\mathbf{A}|\mathbf{b})}{P(\mathbf{G})}, \quad (59)$$

which involves the same marginal likelihood  $P(\mathbf{A}|\mathbf{b})$  we computed previously. With this posterior at hand, we

can proceed by sampling both the partition  $\mathbf{b}$  and the latent multigraph  $\mathbf{A}$  via MCMC. We do so by starting with some initial choice for  $\mathbf{A}$  and  $\mathbf{b}$ , and performing moves of the partition according to a proposal probability  $P(\mathbf{b}'|\mathbf{b})$ , and accepting it with the Metropolis-Hastings [32, 33] probability

$$\min\left(1, \frac{P(\mathbf{A}, \mathbf{b}'|\mathbf{G})P(\mathbf{b}|\mathbf{b}')}{P(\mathbf{A}, \mathbf{b}|\mathbf{G})P(\mathbf{b}'|\mathbf{b})}\right), \quad (60)$$

otherwise we reject the move. Likewise, for a current value of  $\mathbf{A}$  and  $\mathbf{b}$  we also perform move proposals for the latent multigraph with probability  $P(\mathbf{A}'|\mathbf{A})$  and accept it with the analogous criterion

$$\min\left(1, \frac{P(\mathbf{A}', \mathbf{b}|\mathbf{G})P(\mathbf{A}|\mathbf{A}')}{P(\mathbf{A}, \mathbf{b}|\mathbf{G})P(\mathbf{A}'|\mathbf{A})}\right). \quad (61)$$

By alternating between the two kinds of moves, this algorithm will sample asymptotically from the target distribution  $P(\mathbf{A}, \mathbf{b}|\mathbf{G})$ , as long as the move proposals allow us to visit every possible  $(\mathbf{A}, \mathbf{b})$  configuration with nonzero probability. Importantly, when computing the ratios above, it is not necessary to compute the intractable normalization constant  $P(\mathbf{G})$ , as it is the same in the numerator and denominator, and hence cancels out. For the partition move proposal  $P(\mathbf{b}'|\mathbf{b})$ , we use the targeted move proposals described in Ref. [31]. For the multigraph move proposal  $P(\mathbf{A}'|\mathbf{A})$  we choose an edge  $(i, j)$  in  $\mathbf{G}$  uniformly at random, and change the corresponding value of  $A_{ij}$  by summing or subtracting 1 with equal probability, unless that change would make  $A'_{ij} = 0$ , which is forbidden since  $G_{ij} = 1$ . This amounts to

$$P(A'_{ij}|A_{ij}) = \begin{cases} 1 & \text{if } A'_{ij} = 2 \text{ and } A_{ij} = 1, \\ 1/2 & \text{if } A'_{ij} = A_{ij} \pm 1 \text{ and } A_{ij} > 1, \\ 0 & \text{otherwise.} \end{cases} \quad (62)$$

For the DC-SBM model above, a move  $\mathbf{b} \rightarrow \mathbf{b}'$  that changes the group membership of a single node can be done in time  $O(k_i)$  where  $k_i$  is the degree of that node in  $\mathbf{G}$ , independently of how many groups exist in total [31]. The move  $A_{ij} \rightarrow A_{ij} \pm 1$  can be done in constant time  $O(1)$ , as it involves the change of at most a single value of  $e_{rs}$ ,  $e_r$  and  $k_i$  in the likelihood of Eq. 56 for each endpoint of the edge (which remains true when the more advanced priors in Ref. [31] are used instead). Therefore a full sweep of move proposals for each node and edge in  $\mathbf{G}$  can be done in linear time  $O(N + E)$ , which is the best one can hope for this problem, and enables the use of this algorithm for networks with millions of nodes and edges. A reference C++ implementation of the above algorithm is available as part of the `graph-tool` Python library [23].

We emphasize that sampling from the joint posterior  $P(\mathbf{A}, \mathbf{b}|\mathbf{G})$  gives us direct access to the marginal posterior over partitions as well,

$$P(\mathbf{b}|\mathbf{G}) = \sum_{\mathbf{A}} P(\mathbf{A}, \mathbf{b}|\mathbf{G}), \quad (63)$$

which can be obtained with the MCMC algorithm above simply by sampling from the joint distribution, and ignoring the inferred multigraph  $\mathbf{A}$ . So, if we are interested only in the community detection problem, we are well served by this approach. However, obtaining the latent multigraph  $\mathbf{A}$  also has its uses, as we had seen before, for instance in disentangling degree mixing from inherent degree constraints. We can therefore also extract the marginal distribution over edge multiplicities in an analogous way

$$P(\mathbf{A}|\mathbf{G}) = \sum_{\mathbf{b}} P(\mathbf{A}, \mathbf{b}|\mathbf{G}). \quad (64)$$

It is often more convenient to compute the marginal multiplicity distribution over each edge

$$\pi_{ij}(m) = \sum_{\mathbf{A}, \mathbf{b}} \delta_{A_{ij}, m} P(\mathbf{A}, \mathbf{b}|\mathbf{G}), \quad (65)$$

or more simply just its mean value

$$w_{ij} = \sum_{m=0}^{\infty} m \pi_{ij}(m). \quad (66)$$

In the following, we will compare two approaches to community detection: 1. Using the posterior  $P(\mathbf{b}|\mathbf{A})$  based the Poisson multigraph model, considering the simple graph observed as a possible instance; 2. Using the posterior  $P(\mathbf{b}|\mathbf{G})$  based on the erased Poisson model that generates simple graphs exclusively. The original argument given by Karrer and Newman [8] to justify the use of the former approach is that for sparse graphs with an expected number of edges  $E$  that is proportional to the number of nodes  $N$ , the mean parameter of the Poisson distribution will decay as

$$\frac{1}{N^2} \sum_{ij} \theta_i \theta_j \lambda_{b_i b_j} = \frac{2E}{N^2} = O(1/N). \quad (67)$$

If we now consider the probability of observing more than one edge between two nodes  $i$  and  $j$

$$\begin{aligned} \sum_{A_{ij}=2}^{\infty} \frac{(\theta_i \theta_j \lambda_{b_i b_j})^{A_{ij}} e^{-\theta_i \theta_j \lambda_{b_i b_j}}}{A_{ij}!} &= \\ 1 - e^{-\theta_i \theta_j \lambda_{b_i b_j}} - \theta_i \theta_j \lambda_{b_i b_j} e^{-\theta_i \theta_j \lambda_{b_i b_j}} &= \\ \frac{(\theta_i \theta_j \lambda_{b_i b_j})^2}{2} + O[(\theta_i \theta_j \lambda_{b_i b_j})^3], & \quad (68) \end{aligned}$$

we can conclude that it will decay as  $O(1/N^2)$  as long as the corresponding parameters lie close to the mean, which itself decays as  $O(1/N)$ . In this case the probability of observing multiple edges will vanish for large  $N$ , and the model will generate mostly simple graphs. The problem with this argument is that it breaks down precisely when the network is heterogeneous and the parameters  $\theta$  and  $\lambda$  are distributed with a high enough variance. In this

case, despite the vanishing value of the mean, we can in principle have a sizable fraction of products  $\theta_i \theta_j \lambda_{b_i b_j}$  that are arbitrarily high. For example we could have this product approaching 1 for  $N$  node pairs, and as long as the remaining  $O(N^2)$  pairs decay as  $O(1/N)$ , we still have the mean also scaling as  $O(1/N)$ , while the resulting graph would have an abundance of multiedges, despite being globally sparse. Ironically, this is precisely the situation one should expect if the data possess a very strong community structure and very broad degree distributions, making the Poisson model unsuitable. The erased Poisson model, on the other hand, does not rely on uniform sparsity, and should be able to better handle these important scenarios, which we investigate in the following.

## A. Broad degree distributions

We begin illustrating the behavior of the erased Poisson model with the network of political blogs of Adamic and Glance [38], which describes the citations between blogs during the 2004 US elections. Either version of the model finds a wealth of information, dividing the network in many groups. In order to simplify our analysis, we use the known division between liberal and conservative blogs as an imposed partition of randomly generated networks, which we sample from the maximum-entropy DC-SBM of Eq. 48 that preserves the number of edges that go between nodes of the same and different groups, as well as the node degrees, when compared to the real network. This means that, in our analysis, this division is indeed the true one, instead of only putatively true, as is the case of the empirical network. If we now employ the Poisson DC-SBM to the resulting network, we get the partition into five groups, as shown in Fig. 11a. Since the degree constraints induce disassortative degree-degree correlations, something that is not expected with the Poisson model, the inference of that model attempts to account for this pattern by subdividing each group into subgroups of nodes with similar degrees, in an attempt to account for this existing mixing pattern as specific probabilities of connections between these extra groups. If instead we use the erased Poisson model, we uncover correctly only the two planted partitions, as we see in Fig. 11b, as this model is capable of incorporating the induced degree disassortativity intrinsically. Indeed, by inspecting the inferred latent multigraph, we see that it lacks a substantial fraction of the disassortativity, as shown in Fig. 12b, which then only emerges once the multiedges are erased.

## B. Heterogeneous densities

We turn now to a related, but different scenario where the Poisson model also gives suboptimal results. We consider the artificial network composed of a ring of 24 cliques of size 5. This kind of network was used as an ex-

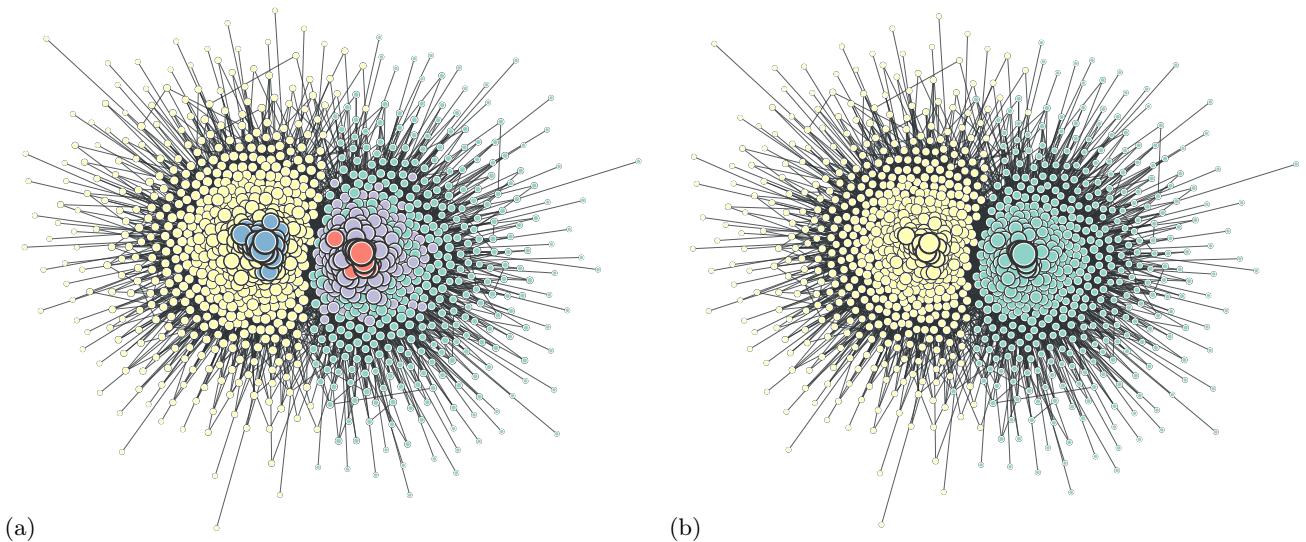


Figure 11. Inferred groups for a political blog network generated from the maximum-entropy DC-SBM, inferred using the (a) Poisson DC-SBM and (b) the erased Poisson DC-SBM, with inferred groups indicated by the node colors, and node degrees by the node sizes. The layout was obtained with the spring-block algorithm of Ref. [34], which tries to place nodes together if they are connected by an edge. The “liberal” and “conservative” groups correspond to the visible left (yellow) and right (blue) clusters, respectively. The layout places nodes with high degree in the center of the figure, which in (a) are clustered into their own separate groups, whereas in (b) they are merged with their true category.

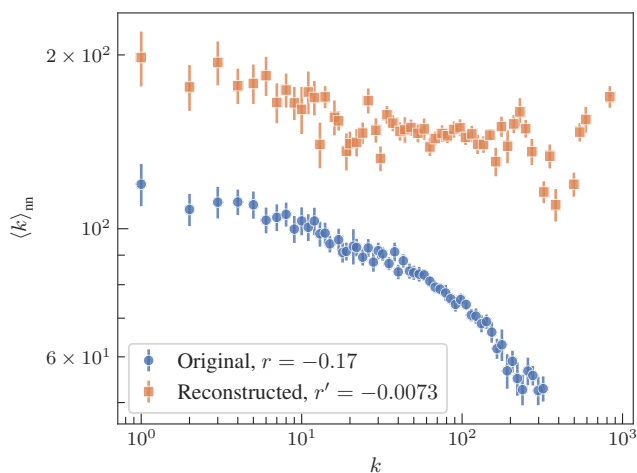


Figure 12. Mean degree of a neighbor of a node of degree  $k$  as a function of  $k$ , for a political blog network generated from the maximum-entropy DC-SBM, and the corresponding inferred latent multigraph.

ample by Good et al [39] of a situation where community detection methods fail to find the more obvious pattern. Indeed, as was shown recently by Riolo and Newman [40], inferring the DC-SBM also yields unsatisfactory results, where adjacent cliques are merged together, as shown in Fig. 13a. In Fig. 14a we see the posterior distribution of effective number of groups, defined as  $B_e = e^{S_e}$ , with

$$S_e = - \sum_r \frac{n_r}{N} \ln \frac{n_r}{N}, \quad (69)$$

being the entropy of the membership distribution. For the DC-SBM above, the posterior distribution fluctuates around 6 groups, falling significantly short of the expected 24.

At first, one might think that this problem is due to an underfitting of the model, caused by the use of non-informative priors. As was shown in Refs. [31, 41], the use of such priors incurs a penalty in the posterior log-probability that grows quadratically with the number of groups, which in turn means that no more than  $O(\sqrt{N})$  groups can ever be inferred in sparse networks. This issue is resolved by replacing the noninformative priors by a deeper hierarchy of priors and their hyperpriors, forming a nested DC-SBM [29]. The use of the nested model, which remains nonparametric and agnostic about mixing patterns, increases the inference resolution by enabling the identification of up to  $O(N/\log N)$  groups. In a similar example of a network composed of 64 cliques of size 10, the nested model is capable of identifying all 64 cliques, whereas the “flat” version finds only 32 groups, composed each of 2 cliques [9].

However, when applied to the current example, the use of the nested Poisson DC-SBM is not sufficient to uncover all 24 cliques. In Fig. 14b we see the posterior distribution of effective group sizes for the nested Poisson model. Although the mean number of groups increases, it still falls short of the 24. This indicates that the problem may be not only underfitting, but also misspecification, i.e. the model is simply not adequate to describe the data. Indeed a closer inspection reveals that this is precisely the case. A version of the DC-SBM that should be able to generate the given number of cliques would

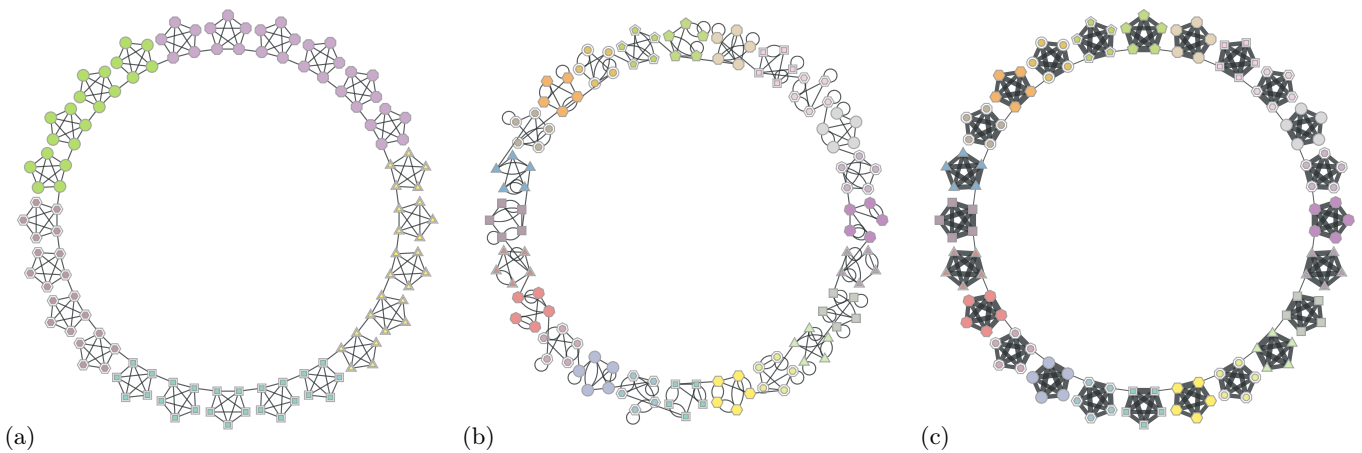


Figure 13. (a) Network composed of a ring of 24 cliques of size 5, connected to each other by a single edge. The node colors and shapes correspond to a typical partition sampled from the posterior distribution of Eq. 52. (b) Network sampled from the maximum-likelihood Poisson DC-SBM obtained from the network in (a) and putting each clique in their own group (as shown by the node colors and shapes). (c) Fit of the erased Poisson nested DC-SBM to the network in (a), showing a sampled partition from the posterior distribution (node shape and color), coinciding perfectly with the individual cliques, and the marginal posterior distribution of edge multiplicities (edge thickness).

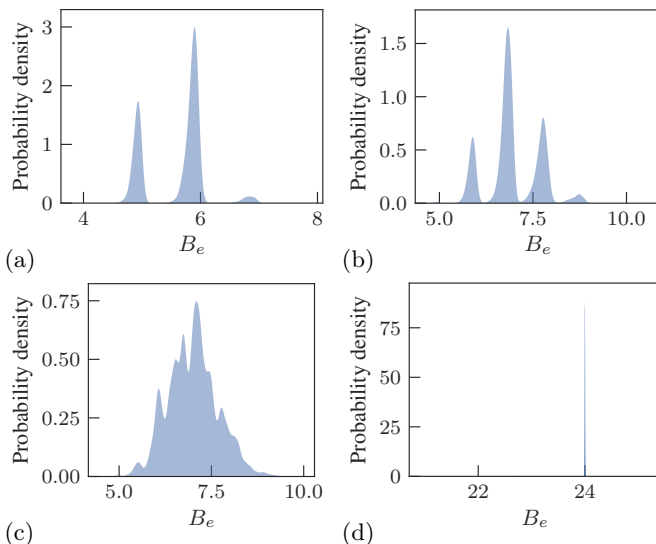


Figure 14. Posterior distribution of effective number of groups  $B_e$  for the network in Fig. 13a, obtained with (a) the Poisson DC-SBM, (b) the nested Poisson DC-SBM, (c) the erased Poisson DC-SBM, and (d) the nested erased Poisson DC-SBM, the latter showing a distribution highly concentrated on  $B_e = 24$ .

be one where the probability of an edge existing between two nodes of the same clique would be very close to one. However, the Poisson model struggles at describing this structure because it cannot allow for a single edge occurring with such a high probability, without generating multiple edges as well. As is illustrated in Fig. 15, the Poisson distribution can generate the occurrence of a single edge with a probability at most  $1/e \approx 0.368$ , and even in that case the occurrence of multiple edges

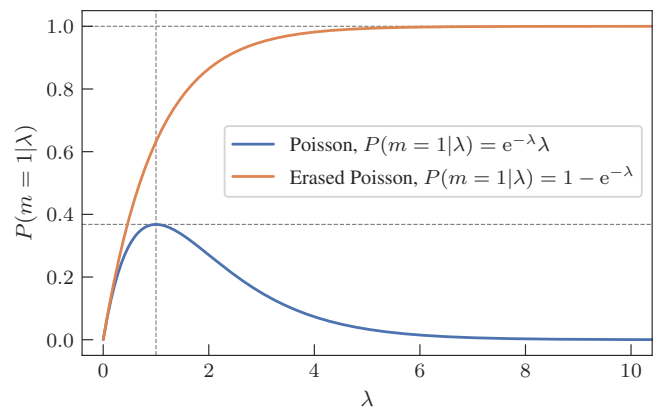


Figure 15. Probability of observing a sample  $m = 1$  from the Poisson and erased Poisson models, as a function of the parameter  $\lambda$ , as shown in the legend. The vertical and horizontal lines show the maximum of the Poisson at  $\lambda = 1$  and  $P(m = 1|\lambda) = 1/e$ , and the asymptotic value of  $P(m = 1|\lambda) \rightarrow 1$  for the erased Poisson model as  $\lambda \rightarrow \infty$ .

is no longer negligible. This limitation is absent from the erased Poisson model, which can describe arbitrary probabilities of single edges. In Fig. 13b we show a sample of the DC-SBM with parameters chosen so that it replicates the original network as closely as possible: the nodes are separated into 24 groups of size 5, the mean number of edges between nodes of the same group is one, and between adjacent groups is  $1/25$ . The resulting network is not only riddled with multiedges and self-loops, but it also shows a far more irregular structure than the original one. However, through the lenses of the Poisson model, both networks are difficult to distinguish, as they have very similar likelihoods. Although it can be possi-

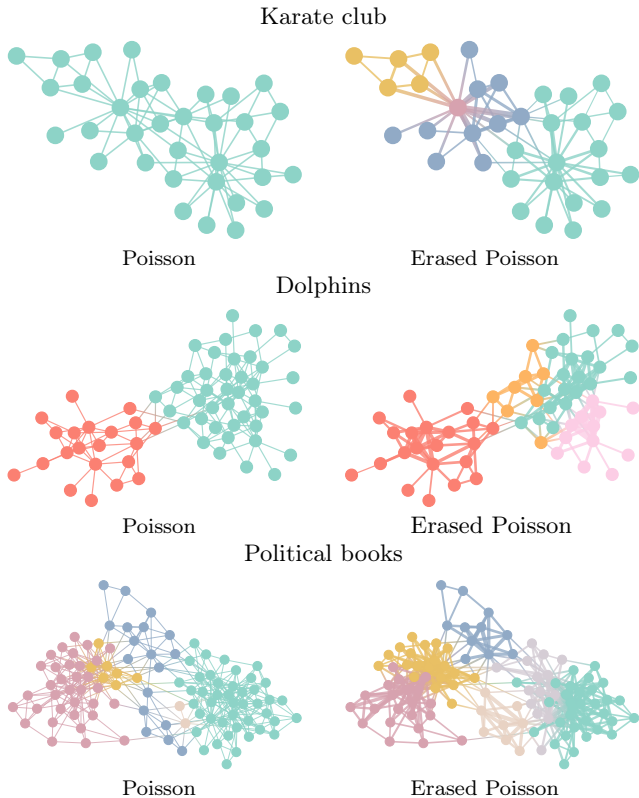


Figure 16. Inferred group memberships for Zachary’s karate club network [35], a dolphin social network [36], and co-purchases of political books [37], using the Poisson DC-SBM and the erased Poisson DC-SBM. In each network, the latter model reveals a larger number of groups, due to its increased ability of identifying heterogeneous densities.

ble to extract useful information even from misspecified models via a detailed inspection of the posterior distribution [40] — a powerful feature of Bayesian methods — this is not a satisfying resolution for such a simple example. Indeed, what we have is once more a situation where the network is globally sparse but locally dense, and we should expect the erased Poisson model to behave better. In fact, using the nested DC-SBM based on the erased Poisson model we can uncover all 24 cliques, as it is capable of describing their probability more accurately. In Fig. 13c is shown the result obtained with the erased Poisson model, together with the inferred latent multigraph, which has a abundance of multiedges inside each group, that translate into cliques once erased, with the probability of each edge approaching one. Importantly, the successful detection of the cliques is only possible if the erased Poisson model is used together with the nested priors of Ref. [31], which illustrates the combined effect of more appropriate model specification with structured priors that prevent underfitting.

We further illustrate the use of the erased Poisson model with some further empirical examples in Fig. 16, comprised of a social network between members of a karate club [35], an animal social network between bot-

tlentose dolphins [36], and co-purchases of books about american politics [37]. In each case, using the erased Poisson DC-SBM we obtain a more detailed division of the network, with a larger number of groups, when compared to the employing the Poisson DC-SBM directly. The most extreme difference is obtained by the karate club network, where the Poisson DC-SBM yields a single group, but the erased Poisson version yields four groups. The explanation for the difference in each case is the same as for the ring-of-cliques example considered previously: since the Poisson DC-SBM is unable to ascribe high probabilities to the existence of edges, it puts a smaller statistical weight to dense regions of the network, even when that would be sufficient to point to the existence of a separate group. The erased Poisson model does not have this limitation and hence is able to isolate this kind of structure with more confidence.

### C. Modularity and group assortativity

An important pattern in network structure is the degree of assortativity, or homophily, between node types. This is commonly measured via the modularity quantity [42], which counts the excess of edges between nodes of the same type, when compared to a null model without any homophily, i.e.

$$Q = \frac{1}{2E} \sum_{i \neq j} (G_{ij} - \langle G_{ij} \rangle) \delta_{b_i, b_j}, \quad (70)$$

where  $\langle G_{ij} \rangle$  is the expectation of an edge  $(i, j)$  existing according to the chosen null model, and the normalization guarantees  $Q \in [-1, 1]$ . The most often used null model is  $\langle G_{ij} \rangle = k_i k_j / 2E$ , which corresponds to a Poisson multigraph model with a maximum-likelihood choice of fugacities  $\theta_i = k_i / \sqrt{2E}$ . As we have discussed, the Poisson model approaches the maximum-entropy simple graph model if the degrees are sufficiently smaller than  $\sqrt{2E}$ , otherwise this assumption becomes inadequate to describe null models of simple graphs. We can use the erased Poisson model as a better alternative in two different ways, the first of which is by simply using its expected value  $\langle G_{ij} \rangle = 1 - e^{-\theta_i \theta_j}$ , which yields

$$\begin{aligned} Q &= \frac{1}{2E} \sum_{i \neq j} [G_{ij} - (1 - e^{-\theta_i \theta_j})] \delta_{b_i, b_j}, \quad (71) \\ &= \frac{1}{2E} \left[ \sum_r e_{rr} - n_r(n_r - 1) + \sum_{i \neq j} e^{-\theta_i \theta_j} \delta_{b_i, b_j} \right], \quad (72) \end{aligned}$$

with  $2E = \sum_{ij} G_{ij}$ . The values of  $\theta$  can be obtained efficiently with the EM algorithm presented in Sec III B. A disadvantage of this approach is that the computation of the last term in the above equation requires  $O[(N/B)^2]$  operations, and thus is not very efficient for large networks. The second approach we describe is faster, and

is comprised of the computation of modularity for the multigraph inferred from  $P(\mathbf{A}|\mathbf{G}, \boldsymbol{\theta})$  using the same EM algorithm (instead of the simple graph  $\mathbf{G}$  directly), for which  $\langle A_{ij} \rangle = \theta_i \theta_j$  becomes the appropriate null model, i.e.

$$Q = \frac{1}{2E'} \sum_{ij} (w_{ij} - \theta_i \theta_j) \delta_{b_i, b_j}, \quad (73)$$

$$= \frac{1}{2E'} \sum_r \omega_{rr} - \hat{\theta}_r^2 \quad (74)$$

$$= \frac{1}{2E'} \sum_r \omega_{rr} - \frac{\omega_r^2}{2E'} \quad (75)$$

with  $2E' = \sum_{ij} w_{ij}$ ,  $\omega_{rs} = \sum_{ij} w_{ij} \delta_{b_i, r} \delta_{b_j, s}$ ,  $\omega_r = \sum_s \omega_{rs}$ ,  $\hat{\theta}_r = \sum_i \theta_i \delta_{b_i, r}$ , and  $\theta_i = \sum_j w_{ji} / \sqrt{2E'}$ . This quantity can be computed in time  $O(E + N)$ , and thus offers a significant speed advantage over the first one. The two approaches are not identical, and we should not expect to obtain the same value of  $Q$  between them in general, but in case the network was in fact sampled from the erased Poisson model, we must have  $Q \approx 0$  with either computation.

We note that the use of modularity maximization with the purpose of identifying communities in networks, although a popular approach, is ill-advised. This is because that method cannot account for the statistical significance of the node partitions found, and can lead to misleading results, such as high-scoring partitions in fully random graphs [43], non-modular networks such as trees [44], has been shown to systematically overfit empirical data [24], while at the same time it will fail for networks with obvious community structure [39, 45]. Nevertheless, if the partitions are obtained with some other method (like the one of we have described in the previous section, which suffers from none of the mentioned shortcomings), or originate from network annotations, the value of  $Q$  can be a good description of the existing homophily, and the corrections above can be used to improve it.

## V. CONCLUSION

We have considered the use of the erased Poisson model to describe simple graphs with different kinds of heterogeneous sparsity, in particular with broad degree distributions and community structure. We have shown how this model can give rise to intrinsic degree-degree correlations that are very similar to those existing in maximum-entropy models of simple graphs. We have presented an expectation-maximization (EM) algorithm to infer the underlying Poisson model from simple graph data, and shown how it can be used to potentially explain observed disassortative degree-degree correlations, if they arise predominantly from the imposed degrees. Previously, this could only have been determined by generating networks from an appropriate null model, and com-

paring the assortativity obtained. Our approach is more constructive, since it yields an inference of a generative model, rather than simply a comparison with a null one. This means it is more informative in situations where the degree constraints can account for only a portion of the correlations observed, in which case our approach yields a residual multigraph, with a subtracted contribution of the degree constraints to the degree correlations, which can be further analyzed in arbitrary ways.

We have also investigated the use of this model in community detection, and shown how it is more adequate to uncover communities not only in simple graphs with broad degree distributions, but also when they possess strong community structure. In the latter case, the erased Poisson model is capable of combining degree correction with the existence of edge probabilities approaching one, meaning it can easily model networks that are globally sparse, but locally dense. The enhanced explanatory power is achieved by sacrificing neither mathematical tractability nor algorithmic efficiency.

The erased Poisson model has been used before as a means to combine multigraph generative models with measurement models for simple graphs, when performing joint network reconstruction with community detection in Refs. [46, 47], although these works omitted a detailed analysis of this modelling approach. Since the erased Poisson model is better specified for networks with strongly heterogeneous density, it remains to be determined to what extent it can improve link prediction and network reconstruction, when compared to alternatives. We leave this investigation for future work.

## Appendix A: Ensemble equivalences

In this section we consider network generative processes that at first might seem distinct, but in fact are equivalent not only to each other but also to the Poisson model considered in the main text.

### 1. Sequential edge-dropping model

We consider the situation where a random multigraph is grown by adding  $E$  edges one by one to the network in sequence, and the probability that a given edge is placed between nodes  $i$  and  $j$  is given by  $q_{ij}$ , with  $\sum_{i < j} q_{ij} = 1$ . In this case, the probability of observing a final multigraph  $\mathbf{A}$  is given by a multinomial distribution

$$P(\mathbf{A}|E) = E! \prod_{i < j} \frac{q_{ij}^{A_{ij}}}{A_{ij}!}. \quad (A1)$$

Now if the total number of edges is also allowed to vary, and it is first sampled from a Poisson distribution with mean  $\lambda$ ,  $P(E) = \lambda^E e^{-\lambda} / E!$ , we have that the marginal

probability will be a product of independent Poisson distributions

$$P(\mathbf{A}) = \sum_E P(\mathbf{A}|E)P(E) \quad (\text{A2})$$

$$= \prod_{i < j} \frac{(\lambda q_{ij})^{A_{ij}} e^{-\lambda q_{ij}}}{A_{ij}!}. \quad (\text{A3})$$

If we make the choice  $q_{ij} = \theta_i \theta_j / \lambda$  and  $\lambda = \sum_{i < j} \theta_i \theta_j$  we recover the Poisson model of Eq. 16, and likewise allowing for self-loops we recover Eq. 18.

This “edge-dropping” process is a simple model of a growing network where the placement of new edges is not affected by the existing edges. While this assumption is likely to be violated in a variety of more realistic settings, the central point here is to notice that it implicitly assumes a distinguishability of the multiedges, due to the order in which they appear. Therefore, a maximum-entropy model that assumes edge distinguishability is the appropriate null model when edges are sampled individually.

## 2. Microcanonical configuration model

The configuration or “stub matching” model is a standard procedure for generating multigraphs with prescribed degree sequences [48, 49]: to each node  $i$  is attributed a number  $k_i$  of distinguishable “stubs” or “half-edges”, which are then paired uniformly at random, allowing for multiedges and self-loops. Since every pairing — or “configuration” — occurs with the same probability, this is a maximum-entropy microcanonical ensemble of configurations (rather than multigraphs), with the prescribed degree sequence functioning as a constraint. This is different from the “canonical” ensembles we have been considering so far, where the degrees are constrained only in expectation. Although the configurations are uniformly distributed, the associated multigraphs are not, since more than one configuration will map to the same multigraph. We can obtain the probability of observing a particular multigraph by enumerating the corresponding configurations. With  $2E = \sum_i k_i$  half-edges, we can count the total number of configurations by starting with any arbitrary half-edge, which can then be paired with  $2E - 1$  other half-edges. For any of these choices, we can pick any of the remaining half-edges which can be paired with any of the other remaining  $2E - 3$  ones. Proceeding in this way we have that the total number of pairings is  $(2E - 1) \times (2E - 3) \times (2E - 5) \times \dots \times 1 = (2E - 1)!!$ . To account for multigraphs, we observe that for each node with  $k_i$  half-edges there are  $k_i!$  permutations of their matchings that yield different configurations but correspond to the same multigraph, if all matched half-edges belong to different nodes. Otherwise, this over-counts  $A_{ij}!$  label permutations of half-edges matched between nodes  $i$  and  $j$ , and likewise  $A_{ii}!!$  permutations for self-loops matched for the same node. Putting all this together, we have that

the multigraphs are distributed according to the ratio

$$P(\mathbf{A}|\mathbf{k}) = \frac{\prod_i k_i!}{(2E - 1)!! \prod_{i < j} A_{ij}! \prod_i A_{ii}!!}, \quad (\text{A4})$$

assuming  $\sum_j A_{ij} = k_i$  for every node  $i$ , otherwise  $P(\mathbf{A}|\mathbf{k}) = 0$ . We note that all generated graphs that happen to be simple with  $A_{ij} \in \{0, 1\}$  occur with the same probability  $\prod_i k_i! / (2E - 1)!!$ . Therefore if we discard all multigraphs, the resulting simple graph ensemble has maximum-entropy (but with a new normalization constant that is intractable in general [50], and even in simpler cases where all  $k_i$  are equal [51]).

For an arbitrary (but in this case necessarily integer) choice of  $k_i = \hat{k}_i$ , this microcanonical ensemble is not equivalent to any of the previous canonical ones, since those allow for fluctuations of the degrees around its imposed expected value. Indeed, this lack of ensemble equivalence persists even in the limit  $N \rightarrow \infty$  [12, 13], unlike more typical situations where the number of imposed constraints is fixed. In the latter case, asymptotic equivalence between ensembles is expected, but since the number of constraints given by Eq. 1 is extensive, i.e. grows with  $N$ , this equivalence is never realized.<sup>2</sup>

In spite of the lack of asymptotic equivalence, an exact equivalence with the Poisson model does exist once we consider the degrees  $k_i$  and fugacities  $\theta_i$  to be unknown random variables, generated by their own models conditioned on a small (non-extensive) number of constraints. For the Poisson model in particular, this scenario is relevant when we observe a network sampled from it, but have no direct information on which values of  $\theta$  were used to generate it.

We begin with the microcanonical model, and assume that the degrees are sampled uniformly at random, constrained only on their total sum,  $2E$ . Since the number of different degree sequences is  $\binom{2E + N - 1}{2E}$ , the uniform probability is

$$P(\mathbf{k}|E) = \binom{2E + N - 1}{2E}^{-1}, \quad (\text{A5})$$

assuming  $\sum_i k_i = 2E$ , otherwise  $P(\mathbf{k}|E) = 0$ . We then assume that the total sum is a sample from a Poisson distribution with mean  $\lambda$ ,  $P(E|\lambda) = \lambda^E e^{-\lambda} / E!$ . This gives us a total marginal distribution

$$P(\mathbf{A}|\lambda) = \sum_{E'} \sum_{\mathbf{k}'} P(\mathbf{A}|\mathbf{k}') P(\mathbf{k}'|E') P(E'|\lambda) \quad (\text{A6})$$

$$= \frac{(2\lambda)^E e^{-\lambda} \prod_i k_i!}{\prod_{i < j} A_{ij}! \prod_i A_{ii}!! (2E + N - 1)!}, \quad (\text{A7})$$

<sup>2</sup> Strictly speaking, the results of Refs. [12, 13] refer to maximum entropy ensembles of simple graphs with hard and soft constraints, but the main arguments are also valid for the configuration and Poisson models.

which is nonzero for every  $\mathbf{A}$ .

Now turning to the Poisson model, we assume without loss of generality the re-parametrization  $\theta_i = \sqrt{2\lambda}\kappa_i$ , with  $\sum_i \kappa_i = 1$  and  $\lambda \in [0, \infty]$ , such that Eq. 18 becomes

$$P(\mathbf{A}|\boldsymbol{\kappa}, \lambda) = \frac{(2\lambda)^E e^{-\lambda} \prod_i \kappa_i^{k_i}}{\prod_{i<j} A_{ij}! \prod_i A_{ii}!!}. \quad (\text{A8})$$

We then assume that  $\boldsymbol{\kappa}$  is sampled uniformly at random from the simplex

$$P(\boldsymbol{\kappa}) = (N-1)! \delta(\sum_i \kappa_i - 1). \quad (\text{A9})$$

Computing the marginal distribution, we obtain

$$P(\mathbf{A}|\lambda) = \int P(\mathbf{A}|\boldsymbol{\kappa}, \lambda) P(\boldsymbol{\kappa}) d\boldsymbol{\kappa} \quad (\text{A10})$$

$$= \frac{(2\lambda)^E e^{-\lambda} \prod_i k_i!}{\prod_{i<j} A_{ij}! \prod_i A_{ii}!!} \frac{(N-1)!}{(2E+N-1)!}, \quad (\text{A11})$$

which is identical to the marginal obtained with the microcanonical model.

The above equivalence means that these two distinct generative processes, involving either the configuration model or the Poisson model, yield exactly the same marginal distribution over multigraphs. A direct consequence of this is that, when all we observe is a single network  $\mathbf{A}$ , there is no information contained in it that allows us to determine whether it came from one of the two models. In statistical terminology, we say these models are not identifiable.

Combining all of the above, we have that the following generative processes are fully identical:

### 1. Poisson model:

- (a) The relative fugacities  $\boldsymbol{\kappa}$  are sampled uniformly at random from Eq. A9.

- (b) Given the expected number of edges  $\lambda$ , the fugacities are given by  $\theta_i = \sqrt{2\lambda}\kappa_i$ , and the network is sampled from the Poisson model of Eq. 18.

### 2. Sequential edge dropping:

- (a) The total number of edges is sampled from a Poisson distribution with mean  $\lambda$ .
- (b) The relative fugacities  $\boldsymbol{\kappa}$  are sampled uniformly at random from Eq. A9.
- (c) The network is sampled from the edge dropping model of Eq. A3, with probabilities  $q_{ij} \propto \kappa_i \kappa_j$  (and allowing for self-loops).

### 3. Configuration model:

- (a) The total number of edges is sampled from a Poisson distribution with mean  $\lambda$ .
- (b) The degrees are sampled uniformly at random from the set that preserves the total number of edges.
- (c) The half-edges are paired uniformly at random.

The above serves to demonstrate that we can arrive at the Poisson model from several simple intuitive assumptions about the network formation mechanism. These are all “null” models of network formation, since they are not meant to realistically explain how networks in the real world are formed, instead they contain only the smallest set of ingredients necessary for a particular pattern — in this case the expected degrees of the nodes. What they all have in common is that, during the network formation, potential multiple edges are treated as individual elements, which is what lies behind the eventual equivalence with the Poisson model.

- 
- [1] Mark Newman, *Networks: An Introduction* (Oxford University Press, 2010).
  - [2] Albert-László Barabási and Réka Albert, “Emergence of Scaling in Random Networks,” *Science* **286**, 509–512 (1999).
  - [3] M. E. J. Newman, “Mixing patterns in networks,” *Phys. Rev. E* **67**, 026126 (2003).
  - [4] Santo Fortunato, “Community detection in graphs,” *Physics Reports* **486**, 75–174 (2010).
  - [5] Juyong Park and M. E. J. Newman, “Origin of degree correlations in the Internet and other networks,” *Physical Review E* **68**, 026112 (2003).
  - [6] Samuel Johnson, Joaquín J. Torres, J. Marro, and Miguel A. Muñoz, “Entropic Origin of Disassortativity in Complex Networks,” *Physical Review Letters* **104**, 108702 (2010).
  - [7] Charo I. Del Genio, Thilo Gross, and Kevin E. Bassler, “All Scale-Free Networks Are Sparse,” *Physical Review Letters* **107**, 178701 (2011).
  - [8] Brian Karrer and M. E. J. Newman, “Stochastic block-models and community structure in networks,” *Physical Review E* **83**, 016107 (2011).
  - [9] Tiago P. Peixoto, “Bayesian Stochastic Blockmodeling,” in *Advances in Network Clustering and Blockmodeling* (John Wiley & Sons, Ltd, 2019) pp. 289–332.
  - [10] E. T. Jaynes, *Probability Theory: The Logic of Science*, edited by G. Larry Bretthorst (Cambridge University Press, Cambridge, UK ; New York, NY, 2003).
  - [11] Ginestra Bianconi, “Entropy of network ensembles,” *Physical Review E* **79**, 036114 (2009).
  - [12] Kartik Anand and Ginestra Bianconi, “Gibbs entropy of network ensembles by cavity methods,” *Physical Review E* **82**, 011116 (2010).
  - [13] Tiziano Squartini, Joey de Mol, Frank den Hollander, and Diego Garlaschelli, “Breaking of Ensemble Equivalence in Networks,” *Physical Review Letters* **115**, 268701 (2011).

- (2015).
- [14] Marián Boguñá, R. Pastor-Satorras, and A. Vespignani, “Cut-offs and finite size effects in scale-free networks,” *The European Physical Journal B - Condensed Matter* **38**, 205–209 (2004).
- [15] Ilkka Norros and Hannu Reittu, “On a conditionally Poissonian graph process,” *Advances in Applied Probability* **38**, 59–75 (2006).
- [16] Marc Barthélemy, “Spatial networks,” *Physics Reports* **499**, 1–101 (2011).
- [17] Ciro Cattuto, Wouter Van den Broeck, Alain Barrat, Vittoria Colizza, Jean-François Pinton, and Alessandro Vespignani, “Dynamics of Person-to-Person Interactions from Distributed RFID Sensor Networks,” *PLOS ONE* **5**, e11596 (2010), publisher: Public Library of Science.
- [18] Henri van den Esker, Remco van der Hofstad, and Gerard Hooghiemstra, “Universality for the Distance in Finite Variance Random Graphs,” *Journal of Statistical Physics* **133**, 169–202 (2008).
- [19] Shankar Bhamidi, Remco van der Hofstad, and Johan van Leeuwen, “Scaling Limits for Critical Inhomogeneous Random Graphs with Finite Third Moments,” *Electronic Journal of Probability* **15**, 1682–1702 (2010).
- [20] Ginestra Bianconi and Albert-László Barabási, “Bose-Einstein Condensation in Complex Networks,” *Physical Review Letters* **86**, 5632–5635 (2001).
- [21] Dong Yao, Pim van der Hoorn, and Nelly Litvak, “Average nearest neighbor degrees in scale-free networks,” arXiv:1704.05707 [math] (2017), arXiv: 1704.05707.
- [22] Clara Stegehuis, “Degree correlations in scale-free random graph models,” *Journal of Applied Probability* **56**, 672–700 (2019).
- [23] Tiago P. Peixoto, “The `graph-tool` python library,” figshare (2014), 10.6084/m9.figshare.1164194, available at <https://graph-tool.skewed.de>.
- [24] Amir Ghasemian, Homa Hosseinmardi, and Aaron Clauset, “Evaluating Overfit and Underfit in Models of Network Community Structure,” *IEEE Transactions on Knowledge and Data Engineering*, 1–1 (2019).
- [25] Jérôme Kunegis, “KONECT: The Koblenz Network Collection,” in *Proceedings of the 22Nd International Conference on World Wide Web, WWW '13 Companion* (ACM, New York, NY, USA, 2013) pp. 1343–1350.
- [26] Jordi Duch and Alex Arenas, “Community detection in complex networks using extremal optimization,” *Physical Review E* **72**, 027104 (2005).
- [27] Lovro Šubelj and Marko Bajec, “Software systems through complex networks science: review, analysis and applications,” in *Proceedings of the First International Workshop on Software Mining, SoftwareMining '12* (Association for Computing Machinery, Beijing, China, 2012) pp. 9–16.
- [28] Reza Zafarani and Huan Liu, *Social computing data repository at ASU* (2009).
- [29] Tiago P. Peixoto, “Hierarchical Block Structures and High-Resolution Model Selection in Large Networks,” *Physical Review X* **4**, 011047 (2014).
- [30] Sergei Maslov, Kim Sneppen, and Alexei Zaliznyak, “Detection of topological patterns in complex networks: correlation profile of the internet,” *Physica A: Statistical Mechanics and its Applications* **333**, 529–540 (2004).
- [31] Tiago P. Peixoto, “Nonparametric Bayesian inference of the microcanonical stochastic block model,” *Physical Review E* **95**, 012317 (2017).
- [32] Nicholas Metropolis, Arianna W. Rosenbluth, Marshall N. Rosenbluth, Augusta H. Teller, and Edward Teller, “Equation of State Calculations by Fast Computing Machines,” *The Journal of Chemical Physics* **21**, 1087 (1953).
- [33] W. K. Hastings, “Monte Carlo sampling methods using Markov chains and their applications,” *Biometrika* **57**, 97–109 (1970).
- [34] Y. Hu, “Efficient, high-quality force-directed graph drawing,” *Mathematica Journal* **10**, 37–71 (2005).
- [35] Wayne W. Zachary, “An Information Flow Model for Conflict and Fission in Small Groups,” *Journal of Anthropological Research* **33**, 452–473 (1977).
- [36] David Lusseau, Karsten Schneider, Oliver J. Boisseau, Patti Haase, Elisabeth Slooten, and Steve M. Dawson, “The bottlenose dolphin community of Doubtful Sound features a large proportion of long-lasting associations,” *Behavioral Ecology and Sociobiology* **54**, 396–405 (2003).
- [37] V Krebs, “Political Books Network,” unpublished, retrieved from Mark Newman’s website: <http://www-personal.umich.edu/~mejn/netdata/>.
- [38] Lada A. Adamic and Natalie Glance, “The political blogosphere and the 2004 U.S. election: divided they blog,” in *Proceedings of the 3rd international workshop on Link discovery, LinkKDD '05* (ACM, New York, NY, USA, 2005) pp. 36–43.
- [39] Benjamin H. Good, Yves-Alexandre de Montjoye, and Aaron Clauset, “Performance of modularity maximization in practical contexts,” *Physical Review E* **81**, 046106 (2010).
- [40] Maria A. Riolo and M. E. J. Newman, “Consistency of community structure in complex networks,” arXiv:1908.09867 [physics] (2019), arXiv: 1908.09867.
- [41] Tiago P. Peixoto, “Parsimonious Module Inference in Large Networks,” *Physical Review Letters* **110**, 148701 (2013).
- [42] M. E. J. Newman and M. Girvan, “Finding and evaluating community structure in networks,” *Physical Review E* **69**, 026113 (2004).
- [43] Roger Guimerà, Marta Sales-Pardo, and Luís A. Nunes Amaral, “Modularity from fluctuations in random graphs and complex networks,” *Physical Review E* **70**, 025101 (2004).
- [44] James P. Bagrow, “Communities and bottlenecks: Trees and treelike networks have high modularity,” *Physical Review E* **85**, 066118 (2012).
- [45] Santo Fortunato and Marc Barthélemy, “Resolution limit in community detection,” *Proceedings of the National Academy of Sciences* **104**, 36–41 (2007).
- [46] Tiago P. Peixoto, “Reconstructing Networks with Unknown and Heterogeneous Errors,” *Physical Review X* **8**, 041011 (2018).
- [47] Tiago P. Peixoto, “Network Reconstruction and Community Detection from Dynamics,” *Physical Review Letters* **123**, 128301 (2019).
- [48] Béla Bollobás, “A Probabilistic Proof of an Asymptotic Formula for the Number of Labelled Regular Graphs,” *European Journal of Combinatorics* **1**, 311–316 (1980).
- [49] B. Fostick, D. Larremore, J. Nishimura, and J. Ugander, “Configuring Random Graph Models with Fixed Degree Sequences,” *SIAM Review* **60**, 315–355 (2018).
- [50] E.A. Bender and J.T. Butler, “Asymptotic Approximations for the Number of Fanout-Free Functions,” *Com-*

puters, IEEE Transactions on **C-27**, 1180–1183 (1978).  
[51] N.C. Wormald, “Models of random regular graphs,” Lon-

don Mathematical Society Lecture Note Series , 239–298  
(1999).